MEMBRANES

# 3D printed polyamide membranes for desalination

Maqsud R. Chowdhury[1], James Steffes[2], Bryan D. Huey[2], Jeffrey R. McCutcheon[1]*

**Polyamide thickness and roughness have been identified as critical properties that affect thin-film composite membrane performance for reverse osmosis. Conventional formation methodologies lack the ability to control these properties independently with high resolution or precision. An additive approach is presented that uses electrospraying to deposit monomers directly onto a substrate, where they react to form polyamide. The small droplet size coupled with low monomer concentrations result in polyamide films that are smoother and thinner than conventional polyamides, while the additive nature of the approach allows for control of thickness and roughness. Polyamide films are formed with a thickness that is controllable down to 4-nanometer increments and a roughness as low as 2 nanometers while still exhibiting good permselectivity relative to a commercial benchmarking membrane.**

The thin-film composite (TFC) membrane has served as the desalination industry's standard membrane for more than 30 years. During that time, this membrane has changed little. The composite structure comprises a polyester backing layer for mechanical support, a porous supporting polysulfone midlayer cast through phase inversion, and an ultrathin, highly cross-linked polyamide film that is dense enough to separate salt ions from water but thin enough to have a low resistance to water transport. This polyamide layer is formed in situ onto the porous midlayer via interfacial polymerization. This approach relies on a reaction between an amine [*m*-phenylene diamine (MPD)] in an aqueous phase and an acid chloride [trimesoyl chloride (TMC)] in an organic phase. The immiscibility of the two phases permit the reaction to occur only at the phase boundary. Film growth is limited to the boundary and subsequently self-limits the reaction as reactants are blocked by the growing film. The result is a self-terminated, but uncontrolled, film growth with a thickness between 100 and 200 nm and a rough ridge-and-valley-like surface morphology (*1*–*3*). Although these membranes exhibit excellent permselectivity compared with any other desalination membrane, certain features of the film properties and its fabrication procedure are inherently limiting. The intrinsic roughness of these films have long been attributed to a high fouling propensity for reverse osmosis and nanofiltration processes (*4*, *5*). Additionally, the thickness of the membrane, which is inversely proportional to its permeance, is relatively uncontrolled because the process simply self-terminates as the film forms. Last, the properties of the support layer surface—including pore size, pore spacing, surface porosity, roughness, and surface chemistry—affect the interface between the two phases and thus the membrane performance in unpredictable ways (*6*–*8*).

A better polyamide desalination membrane should have the same permselective properties as those of existing membranes but also be tunable in each of these other properties. The thickness should be reduced to maximize permeance while still ensuring that the films are sufficiently robust so as to withstand necessary hydraulic pressures. The roughness should be minimized to lessen the likelihood that the membrane will foul and also improve cleaning efficiency. Last, the film properties should be decoupled from the substrate properties, allowing these selective films to be deployed on any type of substrate.

To better control thickness and roughness, Gu *et al.* used a molecular layer-by-layer approach to build polyamide layers onto ultrafiltration (UF) membranes. Using a polyelectrolyte layer to prime the surface of a porous substrate, a polyamide layer could be formed by molecular layer through a sequential interfacial polymerization method (*9*). Karan *et al.* used a sacrificial nanostrand layer as a support to form free-standing polyamide films with varying thickness and roughness for organic solvent nanofiltration applications with no demonstration of desalination performance (*10*). These methods and others (*11*–*16*) are complex and are unlikely to scale easily for commercial production.

Electrospray can be used to deposit monomers as nanoscale droplets that form polyamide onto a substrate. During electrospraying, liquid leaves a needle in the presence of a strong electric field. Coulombic repulsion forces the ejected droplets to disburse with diameters well below 1 μm (Fig. 1, A and B) (*17*). This characteristic drew Fenn *et al.* to use the technique for mass spectrometry of large polar biomolecules (*18*, *19*). Others followed by using the technique to make thin films (*20*–*23*), nanoparticles (*24*), or patterns (*25*–*27*). For our approach, we deposit individual monomers onto a substrate, where they can subsequently polymerize on the surface.

The approach is illustrated in Fig. 1, A and B. The drum is grounded and connected to the two needles by means of a high-voltage dc power source that can generate up to 30 kV. The distance between the needle tip and drum is kept at 2 to 3 cm. Each needle extrudes one of the monomers in solution. MPD (in water) and TMC (in hexane) were kept at a molar ratio of 4:1 over a wide range of concentrations (table S1). A lipophilic ionic liquid was added to the organic phase in order to increase the electrical conductivity (fig. S2A). A variety of UF membrane substrates with different pore sizes (fig. S2B), pure water permeance (fig. S2C), and hydrophilicity were studied (fig. S2D and table S2). In each case, the substrate was first attached to the rotating drum (Fig. 1A). As monomer solutions emerged from the needle tips, they sprayed and deposited onto the collector surface and reacted upon contact with each other. To ensure coverage over the entire substrate, the needle stage traverses along the collector surface (Fig. 1B). A single pass over the collector surface is referred to as a "single scan."

Films were printed on aluminum (Al) foil in order to demonstrate the ability to characterize polyamide films to find properties such as cross-link density, thickness, and mechanical properties. After printing, the films are transferred from the foil (fig. S3A) to any substrate or kept as a free-standing film (Fig. 1C). Having thicker films that can be manipulated by hand allows for easier characterization of film properties. This type of manipulation is difficult with conventional polyamide films because of their thinness, fragility, and integration into the supporting structure of typical TFC membranes. For example, determination of cross-link density of the polyamide film is typically done with x-ray photoelectron spectroscopy (XPS) (*28*). However, this method can be inaccurate because of surface roughness, insufficient sample size, and compositional heterogeneity with depth. Instead, manipulating a 1-μm-thick polyamide into a thicker, crumpled form (fig. S4) allows us to use energy-dispersive x-ray spectroscopy, which penetrates far deeper into the sample and thus provides a better measurement of bulk polyamide composition. The cross-link density is found to be 83%, which is reasonable for a film made from MPD and TMC monomers (fig. S4) (*10*).

Films are also printed at various MPD and TMC concentrations (table S1) onto Al foil and then transferred to a silicon wafer for thickness measurement by using atomic force microscopy (AFM) (fig. S3B). Cross sections at the film edges (fig. S5) reveal the film profile with respect to the underlying planar substrate. Lower monomer concentrations not only result in a thinner polyamide film but also greater control of film thickness per scan. Polyamide films as thin as 20 nm were made based on five scans, indicating a mean thickness of just 4 nm per scan (Fig. 1D). Control of thickness per scan was notably consistent; linearity in film growth with an increasing number of scans is depicted in Fig. 1E.

[1]Department of Chemical and Biomolecular Engineering, University of Connecticut, Center for Environmental Sciences and Engineering, 191 Auditorium Road, Unit 3222, Storrs, CT 06269-3222, USA. [2]Department of Materials Science and Engineering, University of Connecticut, 97 North Eagleville Road, Unit 3136, Storrs, CT 06269-3136, USA.
*Corresponding author. Email: jeffrey.mccutcheon@uconn.edu

Films of the same composition were also printed onto porous polymeric substrates in order to evaluate their thickness, surface morphology, roughness, desalination performance, and substrate independence. Cross-sectional transmission electron microscopy (TEM) images are shown in Fig. 1, F to I, and fig. S6. The polyamide layers printed on the three UF membrane substrates exhibit similar thicknesses (Fig. 1, F to H) as those printed on Al foils (Fig. 1D). We note repeatability in thickness from Fig. 1I, where five layers of polyamide film measuring 15 ± 3 nm each are visible. This thickness per scan corresponds well to thickness per scan data captured on Al foil in Fig. 1D by means of AFM. We also confirm linearity in thickness with TEM images shown in fig. S6.

We examined the surface morphology of the polyamide films formed on polymeric substrates using scanning electron microscopy (SEM) (Fig. 2A and figs. S7 and S8). Compared with the typical ridge-and-valley-like morphology of conventional polyamide films, such as the industry-standard Dow SW30XLE RO membrane (Fig. 2A), significantly smoother polyamide films are formed on all substrates at all monomer concentrations. These results are quantified by means of AFM analysis as shown in Fig. 2B. The root mean square (RMS) roughness increases with increasing monomer concentration (Fig. 2C) and the number of scans (Fig. 2D). For each monomer concentration, film roughness is similar among all of the substrates evaluated (fig. S9 and tables S3 and S4). The maximum roughness (40 ± 4 nm) is observed for the highest MPD:TMC concentration, 0.5:0.3 (Fig. 2C), when formed on the PAN450 UF substrate. However, even these roughest films exhibit less than half of the roughness of the Dow SW30XLE membrane (Fig. 2C, dotted orange overlay). The lowest concentrations of monomers tested here yield films with roughness values of less than 2 nm and are indistinguishable from the substrate's roughness.

The desalination performance for all membranes tested are presented in Fig. 3A, where higher salt rejection and water permeance are desired. Using the SW30XLE as a control and for benchmarking purposes, six of our membranes had both higher rejection and water permeance (within the Fig. 3A gray rectangular overlay), and 30 are higher in one metric or the other. Although it was not the intent of this work to outperform an industry-standard membrane in conventional metrics of water permeance and salt rejection, these membranes can have tailorable thickness and substantially lower roughness while exhibiting comparable (or better, in some cases) performance.

Water permeance (Fig. 3B) and salt rejection (Fig. 3C) are shown to have a strong dependency

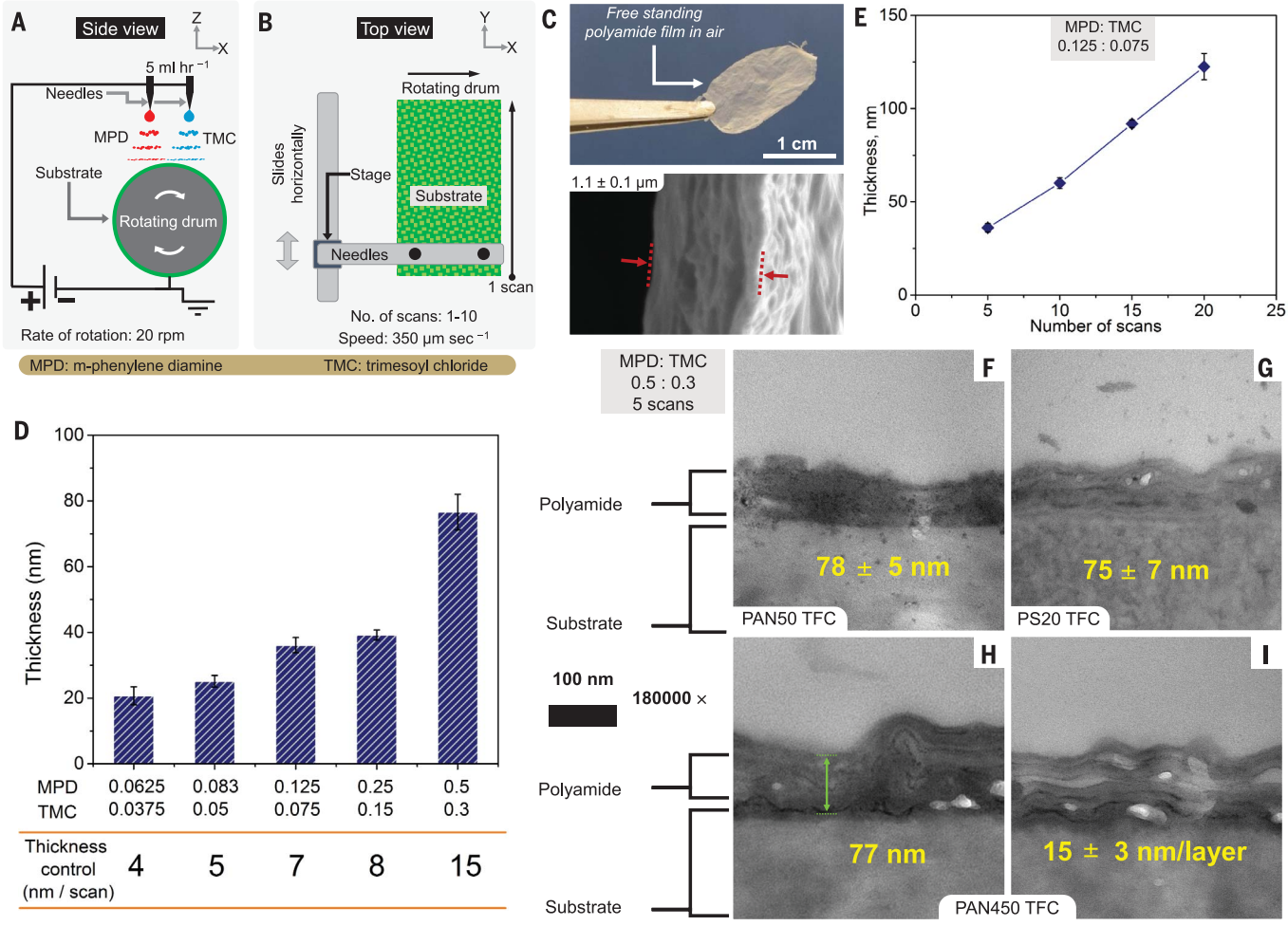


**Fig. 1. Details of the electrospray process for printing substrate-independent polyamide films with thickness control.** (**A**) A side view of a schematic of the electrospray process. (**B**) The top view schematic shows the needles and a stage assembly that can move "horizontally" for uniform coatings on a rotated drum. A single sweep across the substrate is denoted as a single scan. (**C**) A free-standing polyamide film measuring 1.1 μm thick in air, along with the cross-section from SEM. (**D**) Polyamide thickness as a function of MPD and TMC loading, including the corresponding thickness per scan. (**E**) Polyamide thickness as a function of the number of scans at a MPD:TMC concentration ratio of 0.125:0.075. For characterization data presented in (C) to (E), the polyamide was prepared on an Al foil substrate and then separated according to fig. S3A. (**F** to **I**) Cross-section TEM of (F) PAN50, (G) PS20, and [(H) and (I)] PAN450 TFC membranes made with five scans and a MPD:TMC concentration ratio of 0.5:0.3. The displayed thickness and error represents 20 measurements from the images, except for (H), where only the thinnest region is measured.

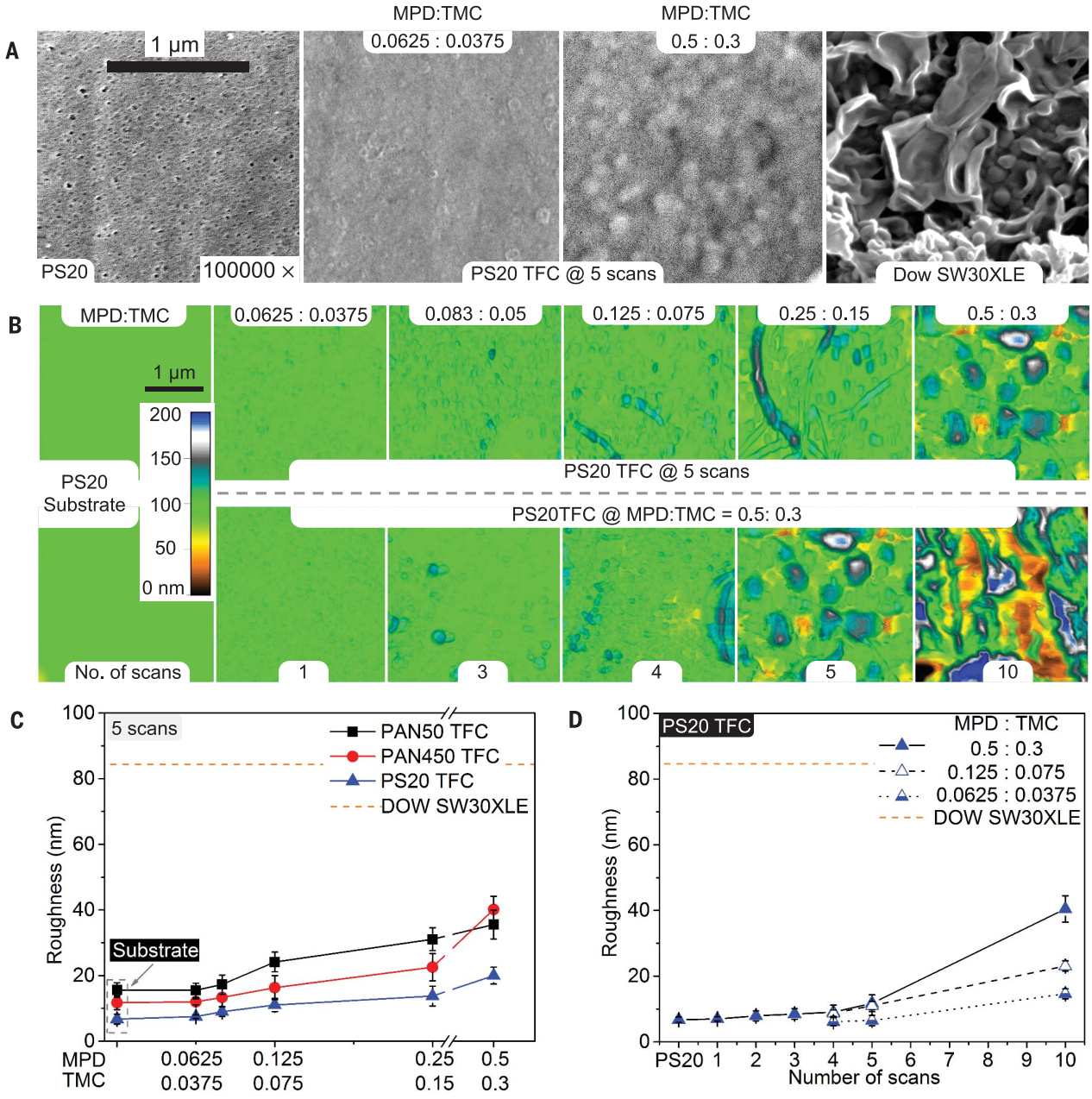


**Fig. 2. Dependency of surface morphology and roughness on printing conditions.** (**A**) SEM image of TFC membranes at 100,000× magnification for different concentrations of MPD and TMC. The underlying substrate and a Dow SW30XLE membrane are shown as controls. (**B**) A series of 3- by 3-μm AFM topography images reveal increased surface roughness with the MPD:TMC concentration ratio, either consistently with five scans (top) or due to successive scans for the specific MPD:TMC concentration ratio of 0.5: 0.3 (bottom). The first column displays the substrate only, without any polyamide film for comparison. The inset numbers indicate either the concentration ratio or the number of scans. (**C**) Graph showing RMS surface roughness of the TFC membranes by using three different UF membranes as substrates for a series of MPD:TMC concentration ratios. The first points in the graph represent the roughness of the substrate only. (**D**) The surface roughness increases with the number of scans for three different MPD:TMC concentration ratios for PS20 TFC membranes. The commercial Dow SW30XLE TFC RO membrane is shown as a dotted line in (C) and (D) for benchmarking.

on monomer concentration. Higher concentrations of monomers form thicker (Fig. 3A) and less permeable films (Fig. 3B) while improving salt rejection (Fig. 3C). The efficacy of the TMC membranes can also be considered by redefining such data in terms of permselectivity, provided in fig. S10, where again these membranes similarly outperform conventional membranes.

The substrate selection has a noticeable effect on permeance. This is attributed to pore size and spacing on the substrate. The most permeable substrate (fig. S2C, PAN 450) exhibits the largest pores that are also closest together. This means that water diffusing through the film has less distance to travel to desorb through an open pore into the porous support, resulting in higher permeance (*6*, *29*, *30*). These higher permeance values enabled our best performing membranes to match the upper-bound limit of the selectivity-permeability tradeoff relationship as described in (*14*) (fig. S11). Furthermore, there was no substrate effect on rejection as expected (Fig. 3C) because rejection is primarily a function of the selective film chemistry and structure. These film

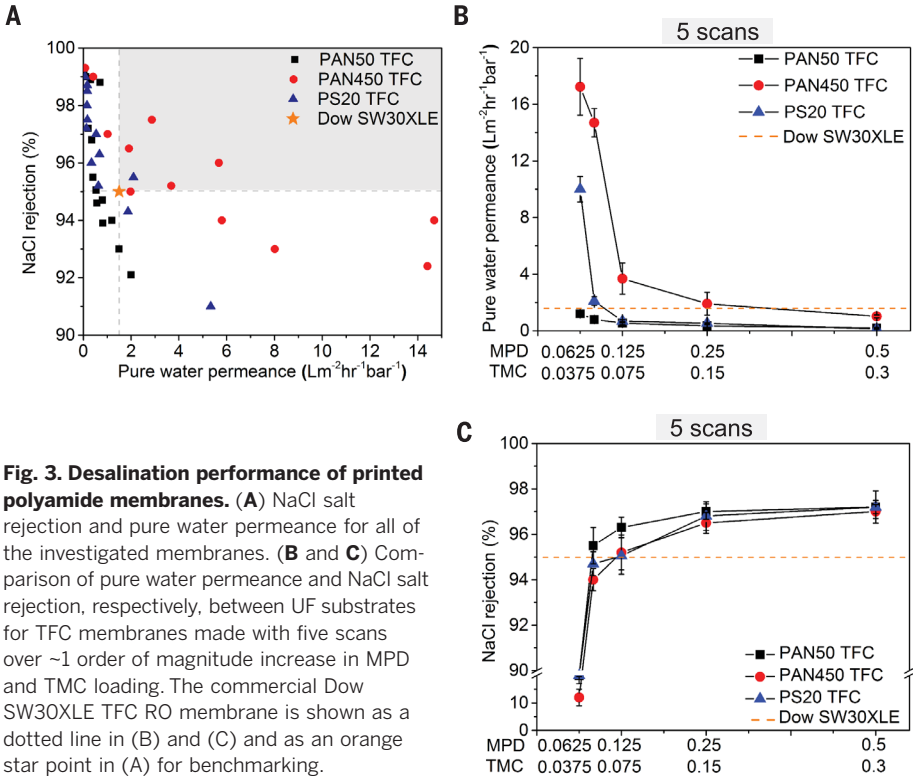


**Fig. 3. Desalination performance of printed polyamide membranes.** (**A**) NaCl salt rejection and pure water permeance for all of the investigated membranes. (**B** and **C**) Comparison of pure water permeance and NaCl salt rejection, respectively, between UF substrates for TFC membranes made with five scans over ~1 order of magnitude increase in MPD and TMC loading. The commercial Dow SW30XLE TFC RO membrane is shown as a dotted line in (B) and (C) and as an orange star point in (A) for benchmarking.

features are indistinguishable when deposited onto the three substrates.

Further tuning of desalination performance is done by changing the number of scans and hence polyamide thickness (fig. S12). Some of the thinnest membranes exhibited very high permeance, although the highest of these has correspondingly low salt rejection (~10%). The TFC membranes made with five scans and an MPD:TMC ratio of 0.083:0.05 on the PAN 450 UF membrane exhibited a reasonable salt rejection of 94%, with a permeance of ~14.7 liter $m^{-2}$ $hour^{-1}$ $bar^{-1}$ (LMH $bar^{-1}$). This membrane also exhibited an RMS roughness only 2.3 nm higher than the substrate RMS roughness of 11.7 nm. This is less than one-sixth that of the SW30XLE membrane. Rejections as high as 95% were achieved on the same substrate for a MPD:TMC ratio of 0.125:0.075, with a RMS roughness only ~4.3 nm greater than that of the substrate and a water permeance of 3.68 LMH $bar^{-1}$. Increasing the number of scans to 10 yielded a salt rejection of 97.5% while still maintaining a water permeance of 2.87 LMH $bar^{-1}$ and a RMS roughness of less than 20 nm.

This additive approach to making TFC membranes has resulted in membranes with tunable thickness and roughness while still retaining the selectivity expected of reverse osmosis membranes. These membranes have an intrinsic smoothness not seen in other TFC membranes today, can be tailored to thicknesses as low as 15 nm with as little as 4-nm resolution in thickness control, and can be formed on substrates without preparation. Furthermore, by decoupling the polyamide formation from the substrate properties, we have enabled the formation of TFCs on unconventional substrates and allowed for film characterization that would be impossible with polyamide films formed through conventional interfacial polymerization. The adaptation of this approach to other monomers or even simple polymers dissolved in solvents might enable the development of other TFC membranes for use in other separations.

## REFERENCES AND NOTES


1. P. W. Morgan, S. L. Kwolek, *J. Polym. Sci. Polym. Phys. Ed.* **XL**, 299–327 (1959).
2. J. E. Cadotte, R. J. Petersen, R. E. Larson, E. E. Erickson, *Desalination* **32**, 25–31 (1980).
3. J. E. Cadotte, Interfacially synthesized reverse osmosis membrane, U.S. patent 4,277,344 (1981).
4. M. Elimelech, W. A. Phillip, *Science* **333**, 712–717 (2011).
5. A. D. Khawaji, I. K. Kutubkhanah, J. M. Wie, *Desalination* **221**, 47–69 (2008).
6. A. K. Ghosh, E. M. V. Hoek, *J. Membr. Sci.* **336**, 140–148 (2009).
7. V. Freger, *Langmuir* **19**, 4791–4797 (2003).
8. V. Freger, *Environ. Sci. Technol.* **38**, 3168–3175 (2004).
9. J. E. Gu *et al.*, *Adv. Mater.* **25**, 4778–4782 (2013).
10. S. Karan, Z. Jiang, A. G. Livingston, *Science* **348**, 1347–1351 (2015).
11. W. Choi *et al.*, *J. Membr. Sci.* **527**, 121–128 (2017).
12. X. Song, S. Qi, C. Y. Tang, C. Gao, *J. Membr. Sci.* **540**, 10–18 (2017).
13. S.-J. Park *et al.*, *J. Membr. Sci.* **526**, 52–59 (2017).
14. T. Tsuru *et al.*, *J. Membr. Sci.* **446**, 504–512 (2013).
15. X.-H. Ma *et al.*, *Environ. Sci. Technol. Lett.* **5**, 117–122 (2018).
16. X.-H. Ma *et al.*, *Environ. Sci. Technol. Lett.* **5**, 123–130 (2018).
17. A. E. Seaver, C. J. Eckhardt, Electrospray coating process, U.S. patent 4,748,043 (1988).
18. J. B. Fenn, M. Mann, C. K. Meng, S. F. Wong, C. M. Whitehouse, *Science* **246**, 64–71 (1989).
19. J. B. Fenn, M. Mann, C. Meng, S. Wong, C. M. Whitehouse, *Mass Spectrom. Rev.* **9**, 37–70 (1990).
20. R. Saf *et al.*, *Nat. Mater.* **3**, 323–329 (2004).
21. I. B. Rietveld, K. Kobayashi, H. Yamada, K. Matsushige, *Soft Matter* **5**, 593–598 (2009).
22. J. Sakata, M. Mochizuki, *Thin Solid Films* **195**, 175–184 (1991).
23. K. Morota *et al.*, *J. Colloid Interface Sci.* **279**, 484–492 (2004).
24. A. Jaworek, *Powder Technol.* **176**, 18–35 (2007).
25. J.-U. Park *et al.*, *Nat. Mater.* **6**, 782–789 (2007).
26. A. Jaworek, A. T. Sobczyk, *J. Electrost.* **66**, 197–219 (2008).
27. Y. K. Hwang, U. Jeong, E. C. Cho, *Langmuir* **24**, 2446–2451 (2008).
28. C. Y. Tang, Y. N. Kwon, J. O. Leckie, *J. Membr. Sci.* **287**, 146–156 (2007).
29. J. Mulder, *Basic Principles of Membrane Technology* (Springer Netherlands, ed. 2, 1996).
30. H. B. Park, J. Kamcev, L. M. Robeson, M. Elimelech, B. D. Freeman, *Science* **356**, eaab0530 (2017).


## ACKNOWLEDGMENTS


The authors acknowledge M. Abril and X. Sun of Biosciences Electron Microscopy Facility at the University of Connecticut for performing TEM analysis. The SEM studies were performed by using the facilities in the University of Connecticut/Thermo Fisher Scientific Center for Advanced Microscopy and Materials Analysis (CAMMA). **Funding:** This work was supported by a University of Connecticut graduate teaching assistantship, General Electric Graduate Fellowship for Innovation, NSF DMR:MRI award 1726862, U.S. EPA grant RD834872, and the University of Connecticut Academic Plan funding program. **Author contributions:** All of the system design work, method development, model development, membrane fabrication, characterization, and testing were carried out by M.R.C. Experimental plan and theory were developed by M.R.C. and J.R.M. J.S. and B.D.H provided AFM instruments, advice, training, experimental design assistance, and data analysis, and M.R.C. performed the experiments. **Competing interests:** M.R.C. and J.R.M. are inventors on a provisional patent application (U.S. 62/538503) submitted by University of Connecticut. **Data and materials availability:** All data needed for the conclusions made in this work are reported in the main text or the supplementary materials.


## SUPPLEMENTARY MATERIALS

www.sciencemag.org/content/361/6403/682/suppl/DC1
Materials and Methods
Figs. S1 to S12
Tables S1 to S4
References (*31–46*)


28 October 2017; accepted 8 June 2018
10.1126/science.aar2122

# 3D printed polyamide membranes for desalination

Maqsud R. Chowdhury, James Steffes, Bryan D. Huey and Jeffrey R. McCutcheon

*Science* **361** (6403), 682-686.
DOI: 10.1126/science.aar2122

**Spraying makes it smoother**

Commercial reverse osmosis processes for water desalination use membranes made by the polymerization of polyamide at the oil/water interface. Chowdhury *et al.* show that thinner, smoother membranes can be made with an electrospray technique. Using high voltage, the two precursors are finely sprayed onto a substrate and polymerize on contact. The composition of the resulting membrane can be tuned on the basis of the proportion of the two components. At optimum conditions, the membranes appear to be better at desalination than current commercial reverse osmosis membranes.

*Science*, this issue p. 682